Food Chemistry 121 (2010) 372–380

Contents lists available at ScienceDirect

Food Chemistry

journal homepage: www.elsevier.com/locate/foodchem

Morphology, profile and role of chelate-soluble pectin on tomato properties during ripening

Ying Xin [a], Fusheng Chen [a], Hongshun Yang [a,*], Penglong Zhang [a], Yun Deng [b], Bao Yang [c]

[a] College of Food Science and Technology, Henan University of Technology, 140 S Songshan Rd, Zhengzhou, Henan 450052, China
[b] Department of Food Science and Technology, College of Agriculture and Biology, Shanghai Jiao Tong University, 800 Dongchuan Rd., Minhang, Shanghai 200030, China
[c] South China Botanical Garden, Chinese Academy of Sciences, Guangzhou 510650, China

ARTICLE INFO

Article history:
Received 20 September 2009
Received in revised form 8 November 2009
Accepted 9 December 2009

Keywords:
Atomic force microscopy (AFM)
Tomato
Firmness
Monosaccharide composition
Pectin

ABSTRACT

To illustrate the role of chelate-soluble pectin (CSP) on fruit properties, neutral sugar composition and morphology of CSP from two tomato cultivars ('Dongsheng' and 'Geruisi') at two ripening stages (turning and light-red) were investigated by high-performance liquid chromatography (HPLC) and atomic force microscopy (AFM), respectively. Physicochemical properties and firmness of the tomatoes were determined as well. The percentage of wide CSP chains was reduced and the large CSP polymers were found degraded more with lower firmness during ripening. The proportion of galacturonic acid (GalUA) and rhamnose (Rham) increased during tomato ripening in both cultivars. The proportion of xylose (Xyl) and arabinose (Ara) increased in 'Dongsheng' tomatoes while decreased in 'Geruisi'. The results indicate that the morphology and neutral sugar composition of CSP were closely related with firmness of tomatoes.

1. Introduction

Plant pectin is one of the major contributors for maintaining the texture of fruits and vegetables. It is enriched in the cell middle lamella and cellular junctions which are thought to largely contribute to cell–cell adhesion and tissue cohesion, while the cellulose–hemicellulose network play a role in rigidity. As pectin is an important component for texture, the degradation of pectin would affect fruit ripening. The degradation leads to the disassembly of cellulose–hemicellulose network and accelerates the fruit softening rate (Duan et al., 2008).

Pectins are complex polysaccharides that are generally described as containing different structural domains: homogalacturonan (HG), type I rhamnogalacturonan (RG I) and type II rhamnogalacturonan (RG II). HG contains contiguous (1–4)-α-linked galacturonic acid (GalUA), which has 100–200 GalUA residues (Bonnin, Dolo, Le Goff, & Thibault, 2002). 1,4-α-linked GalUA interrupted by the insertion of 1,2-α-linked rhamnose (Rha) formed the RG I, which is mainly composed of 1,4-β-D-galactan and/or 1,5-α-L-arabinan as neutral sugar side chains. RG II has a very complicated structure, of which galacturonan is replaced by diverse sugars and linkages (Willats, McCartney, Mackie, & Knox, 2001; Yang, Lai, An, & Li, 2006b). The monosaccharide compositions of pectin can be determined by high-performance liquid chromatography (HPLC).

Atomic force microscopy (AFM) has been utilized to illustrate the nanostructural information of fruit polysaccharide molecules, including directly imaging pectin from unripe tomatoes (Kirby, MacDougall, & Morris, 2008; Round, Rigby, MacDougall, Ring, & Morris, 2001) and pectin–protein complex (Kirby et al., 2008). Pectins from peaches (Yang, et al., 2006b; Yang, Feng, An, & Li, 2006a) and cherries (Zhang et al., 2008), the branching of pectin from marsh cinquefoil (Ovodova et al., 2006) were also characterized by AFM successfully. The nanostructure of the polysaccharides provides useful information of physicochemical and texture of food materials.

However, the characterisation of polysaccharides on the nanoscale only provides general structural information about fruit cell walls. Results of monosaccharide compositions cannot help illustrate the general structural changes of fruit cell walls. On the other hand, with the combination of monosaccharide compositions and the characterisation of polysaccharide structure, more information of quality changes of fruit during postharvest will be identified. While both CSP and sodium carbonate–soluble pectin were related to the textural changes of postharvest fruits (Yang et al., 2006a; Zhang et al., 2008), CSP was chosen since it was viewed as responsible for the textural evolution of fruits through depolymerisation (Brummell, 2006).

Tomato (*Lycopersicon esculentum* Mill.) is a climacteric fruit in which ripening is accompanied by softening and physicochemical

* Corresponding author. Tel.: +86 371 67789991; fax: +86 371 67756856.
E-mail address: hongshunyang@hotmail.com (H. Yang).

0308-8146/$ - see front matter © 2009 Elsevier Ltd. All rights reserved.
doi:10.1016/j.foodchem.2009.12.038

changes. The pectin changes during tomato ripening which might be associated with the texture of fruits, one important quality factor of the fruit shelf-life and commercial value (Almeida & Huber, 2008; Lenucci, Leucci, Piro, & Dalessandro, 2008; Zhang et al., 2008). So far, much of the work in the area of tomato ripening has been focused on extending tomato consistency, colour and shelf-life (Martínez-Romero et al., 2009). The mechanism by which tomatoes soften among ripening stages or cultivars is not fully illustrated.

In this manuscript, tomato was selected as the object of study. The aim is to illustrate the mechanism of tomato softening and help build a solid theoretical direction for fruit distributors as well as postharvest researchers. The role of neutral sugar composition and nanostructure of CSP in ripening of tomatoes was investigated. Two tomato cultivars (crisp and soft) at different maturity levels were chosen for a comparative study. The degradation mechanism of the tomato CSP was proposed.

2. Materials and methods

2.1. Fruit materials

Two tomato (*Lycopersicon esculentum* Mill.) cultivars (crisp 'Dongsheng' and soft 'Geruisi') were applied for the experiment. The two ripening stages (turning stage and light-red stage) classified by a colour chart, were selected by experienced farmers (Getinet, Seyoum, & Woldetsadik, 2008). The two cultivars were picked by hand at a farm in Zhengzhou, Henan province, China. The tomatoes were transported to the laboratory within 2 h after harvest. Disease free fruits were sorted according to uniform size, colour, shape and absence of external injury, and were subjected to washing with tap water and wiping free of surface moisture.

2.2. Firmness measurement

Fruit firmness was determined with a TA-XT2i texture analyzer (Stable Micro Systems Ltd., Godalming, Surrey, UK) with the method described by Lien, Ay, and Ting (2009) with slight modifications. Whole tomato with skin and pit but without stem was used. Ten fruits were measured without destruction for each sample. A cylindrical probe (diameter = 10 cm) was applied. The tested speed was set at 1.0 mm/s and pressed distance set at 2 mm. The maximum value of the force was recorded as firmness.

2.3. Titratable acidity and total soluble solid content

The titratable acidity (TA), as percent citric acid, was assayed by indicator titration of 50 ml diluted juice (50 ml of pressed tomato juice were diluted to 250 ml with distilled water) with 0.1 M NaOH. Phenolphthalein was used as indicator and the titration was terminated when the colour of the solution changed to pink without fading in 30 s. The results were expressed as g of citric acid equivalent per g of fresh weight (FW). Ten fruits were randomly used for measuring total soluble solids (TSS) content of each lot. TSS content was assayed using a digital refractometer (WYT-J, Sichuan, China) at 20 °C. The result of TSS was expressed as °Brix (Zhang et al., 2008).

2.4. Cell wall preparation and CSP determination

Cell wall material of tomato flesh was extracted with the methods described by Zhang et al. (2008) with slight modifications. Peeled tomato flesh (10 g) was cut and boiled in 200 ml of 80% (v/v) ethanol for 20 min to inactivate potential cell wall modifying enzymes. The sample was filtrated using a vacuum pump after being cooled to room temperature. Then the same procedure was repeated two more times. Next, the residue was incubated overnight at 4 °C with 50 ml dimethysulphoxide (DMSO, Tianjin Resent Chemical Co., Ltd, China): water (9:1, v/v) for removing starch. Subsequently, the sample was transferred to 200 ml of chloroform: ethanol (2:1, v/v). After 10 min, it was filtrated and washed using 200 ml acetone until total whitening. This residue was cell wall material.

The cell wall material was then suspended in 10 ml ultra purified water, shaken for 4 h at 25 °C, and centrifuged at 10,000*g* at 4 °C for 10 min (Shanghai Anting Scientific Instrument Factory, Shanghai, China). The procedure was repeated two more times, the residue was resuspended in 10 ml of 50 mM cyclohexane-trans-1,2-diamine tetra-acetate (CDTA, Tianjin Zinco Fine Chemical Institute, China), shaken for 4 h, and centrifuged as described previously. The supernatant was collected and the residue was re-extracted twice with CDTA. All supernatants were collected together as the fraction of chelate-soluble pectin (CSP).

The CSP content of tomato was assayed with the Carbazole colourimetry method (Zhang et al., 2008). Galacturonic acid (Sigma–Aldrich Co., Ltd., St. Louis, MO, USA) was used as standard. CSP solution (2 ml) was combined with 12 ml of sulfuric acid (98%, w/w) in a test tube, mixed and cooled with ice water immediately, boiled for 10 min and then cooled with running tap water. Carbazole ethanol solution (0.5 ml) was added to the solution, mixed and incubated at room temperature for 30 min, then the absorbance at 530 nm (A_{530nm}) was determined using a UV-2000 spectrophotometer (Unico Instrument Co. Ltd., Shanghai, China) at room temperature. The CSP solution could be diluted for matching the result of standard galacturonic acid. All experiments were conducted in triplicate and results were expressed as mg of galacturonic acid per g of FW.

2.5. Neutral sugar composition of CSP analysis by HPLC

The neutral sugar composition of CSP was analyzed by HPLC using the methods described by Fu and O'Neill (1995) with some modifications. CSP solution (5 ml) was dissolved in 2 ml of 2 M trifluoroacetic acid, then hydrolyzed at 121 °C for 2 h. After being cooled to room temperature, each reaction mixture was transferred to a micro-centrifuge tube and then freeze-dried. The dried sample was labeled directly with 1-phenyl-3-methyl-5-pyrazolone (PMP) by adding 100 μl of PMP solution (0.5 M in methanol) and 100 μl of sodium hydroxide solution (0.3 M), mixed and incubated at 70 °C for 2 h. PMP was used for quantitative determination of the neutral sugar composition since it reacted with the neutral sugar composition and the resulted derivative could be quantitatively determined by spectrometry or an electrochemical detector (Honda et al., 1989). Then the mixture was neutralized by adding 100 μl of hydrochloric acid solution (0.3 M). Chloroform (0.5 ml) was then added and mixed thoroughly by vortexing. After the organic phase was carefully removed and discarded, the extraction process was repeated two more times. The resulting aqueous phase was added to 1 ml with distilled water and mixed for HPLC analysis.

Analysis of the PMP-labeled neutral sugar compositions was carried out on a HPLC system (Model 1100, Agilent Technologies Inc., Santa Clara, CA, USA). A C-18 column, 4.6 × 250 mm, 5 μm, optimized for the separation of PMP-labeled carbohydrates, was applied with the mobile phase of 0.1 mol/l phosphate buffer (pH 6.7)-acetonitrile (83:17, v/v). The flow rate was 1 ml/min and the wavelength of UV detection was 254 nm. Individual sugars were identified by comparing the retention time with that of standards.

2.6. Nanostructural characterisation and analysis

The nanostructure of CSP was analysed with a Multimode NanoScope IIIa AFM (Digital Instruments, Santa Barbara, CA, USA) equipped with an E(J) scanner (Liu et al., 2009). AFM was conducted with tapping mode in a glove box with 30–40% of relative humidity

at about 25 °C. The relative humidity inside the glove box was adjusted and stabilized by silica gel before examining the samples.

Pectin solution was diluted to about 10 μg/ml and votexed with a XW-80A Vortex mixer (Shanghai Jinke Co., Ltd., Shanghai, China). Then it was pipetted rapidly onto the freshly cleaved mica surface. The mica surface was then dried by forced air using an ear syringe, which had a similar effect as molecular manipulation on pulling out the pectin molecules from the solution. The imaging was conducted in air with a scan speed of 2 Hz. The scanner was adjusted to select and capture smaller areas within the region that is capable of scanning (Yang et al., 2006b). NSC 11/No Al tip was used with resonance and a force constant of 330 kHz and 48 N/m, respectively.

AFM images were analyzed offline using the AFM software (Version 5.30r3sr3) provided by the company. After the noise of the samples was reduced through the function of flattening of the software, high quality images were then obtained. The bright and dark areas in the AFM images corresponded to high and low parts in the observed CSP samples. It should be noted that different scales were applied in the vertical (about several microns) and horizontal axes (about several nanometers), and height mode images for each group were used for the analysis (Yang et al., 2006a).

Both qualitative and quantitative information could be obtained. The chain features of CSP could be characterized, including cleavage points, long chain, linear single fractions, polymers and short chains. The dimensions (width and height) of the pectin molecules were obtained using section analysis of the AFM software before flattening the images. The length of pectin chain was determined by plotting the main chain with the software. The width and height of a single strand was determined by measuring the horizontal distance and vertical distance, respectively (Yang et al., 2006b). The number of specific chain widths was recorded as frequency (*Fq*) (Liu et al., 2009).

2.7. Statistical analysis

Sample preparation and measurements of TA, CSP contents and neutral sugar compositions were determined in triplicate. Ten replicates for TSS and firmness. At least ten AFM images were analyzed for each condition. The zoom images of marked square in large area images were not included in the statistics. Statistical analyses using analysis of variance (ANOVA) ($P < 0.05$) and Duncan's multiple range tests for differences in the quantitative dimensions of pectin chains were performed using SAS software (Version 9.1.3, SAS, Cary, NC, USA). Data of physicochemical properties and vertical distances of vertical CSP chains were expressed as mean ± standard deviation. Comparisons that yielded $P < 0.05$ were considered significant.

3. Results and discussion

3.1. Effects of ripening stages and cultivars on the firmness and physicochemical properties of tomatoes

Effects of ripening stages and cultivars on the firmness and physicochemical properties of tomatoes were shown in Table 1. Firmness was one of the most important factors that affected the storage properties of fruits and vegetables. The decrease in firmness during tomato ripening was reported in many studies (Lana, Tijskens, & Kooten, 2005; Mizrach, 2007). The different rate of softening and firmness were characteristics of cultivars (Muskovics, Felföldi, Kovács, Perlaki, & Kállay, 2006). In both cultivars, the firmness shows statistical differences between the two ripening stages at $P < 0.05$. Take the 'Dongsheng' groups, for instance: the firmness of the turning stage group was 35.5 N while the light-red stage group was 26.8 N. There was statistical difference between the two cultivars groups in the light-red ripe group (26.8 N for 'Dongsheng' and 23.5 N for 'Geruisi') as well. This shows that the firmness of 'Dongsheng' tomato was larger than that of the soft 'Geruisi' cultivar at the same ripening stages.

For TA and TSS contents, the results reveal that there was a significant ($P < 0.05$) effect of ripening stages and cultivars on the changes of TA and TSS content of tomatoes (Table 1). The TA content of tomatoes decreased with tomato ripening, however the TSS increased. For the 'Dongsheng' group, the TA of the turning stage group was 0.31% and the light-red stage group was 0.16%, the TSS of the turning and light-red stage groups were 3.29 and 4.08 °Brix, respectively. For the 'Geruisi' group, the TA were 0.56% and 0.41%, and TSS were 4.59 and 5.05 °Brix, respectively. The two cultivars had similar changing patterns, which was in accordance with other reports (Artés, Conesa, Hernández, & Gil, 1999). And there were significant differences between the two cultivars, and between the two ripening stages. The TA of the 'Dongsheng' groups was higher than that of the 'Geruisi' groups. Some recent studies had shown that TSS was positively correlated to TA among cultivars. The positive correlation between TSS (sugars) and TA means that plants with high sugars generally have more free organic acids simultaneously (Saliba-Colombani, Causse, Langlois, Philouze, & Buret, 2001). TA content of tomatoes decreased during ripening because of it being a substrate in respiration process. The reason that TSS content increased was that starch and other polysaccharides were hydrolyzed during ripening (Javanmardi & Kubota, 2006).

The CSP content increased with the ripening of tomato fruit in both cultivars (Table 1). During ripening, the CSP content increased from 0.40 to 0.43 mg g^{-1} FW^{-1} for the 'Dongsheng' cultivar, and from 0.36 to 0.41 mg g^{-1} FW^{-1} for the 'Geruisi' cultivar. The CSP contents of the 'Dongsheng' fruits were higher than those of the corresponding 'Geguisi' fruit. Table 1 also reveals that the content of CSP increased while the firmness decreased during ripening in both cultivars. The increase in CSP has been observed in many fruits during ripening including tomato, probably coming from the fraction of sodium carbonate-soluble pectin. This increased amount of CSP suggests that during ripening a proportion of pectin that originally attached to the cell wall through covalent bonds detached since the bonds become weaker and weaker during ripening (Brummell, 2006).

3.2. Effects of ripening stages and cultivars on the neutral sugar composition of CSP

Fig. 1 shows the HPLC images of monosaccharides from standard and tomato CSPs. Table 2 shows the results of neutral sugar composition of tomato CSP from different cultivars and ripening

Table 1
Effects of ripening stages and cultivars on firmness and physiochemical properties of tomatoes[e].

Group	Firmness (N)	TA (%)	TSS (°Brix)	CSP (mg g^{-1} FW^{-1})
Turning stage 'Dongsheng'	35.5 ± 6.2a	0.31 ± 0.01c	3.29 ± 0.62d	0.40 ± 0.02a
Light-red stage 'Dongsheng'	26.8 ± 2.8b	0.16 ± 0.01d	4.08 ± 0.33c	0.43 ± 0.01a
Turning stage 'Geruisi'	32.6 ± 3.7a	0.56 ± 0.02a	4.59 ± 0.34b	0.36 ± 0.02b
Light-red stage 'Geruisi'	23.5 ± 2.1c	0.41 ± 0.00b	5.05 ± 0.46a	0.41 ± 0.03a

[e] The values that have different letters in the same column are significantly ($P < 0.05$) different.

stages. The results reveal that the CSP of tomatoes was composed of an abundance of GalUA, which was in accordance with Kirby et al. (2008). Glucose (Glc) and galactose (Gal) were the most abundant noncellulosic neutral sugars in tomato CSP, followed by arab-

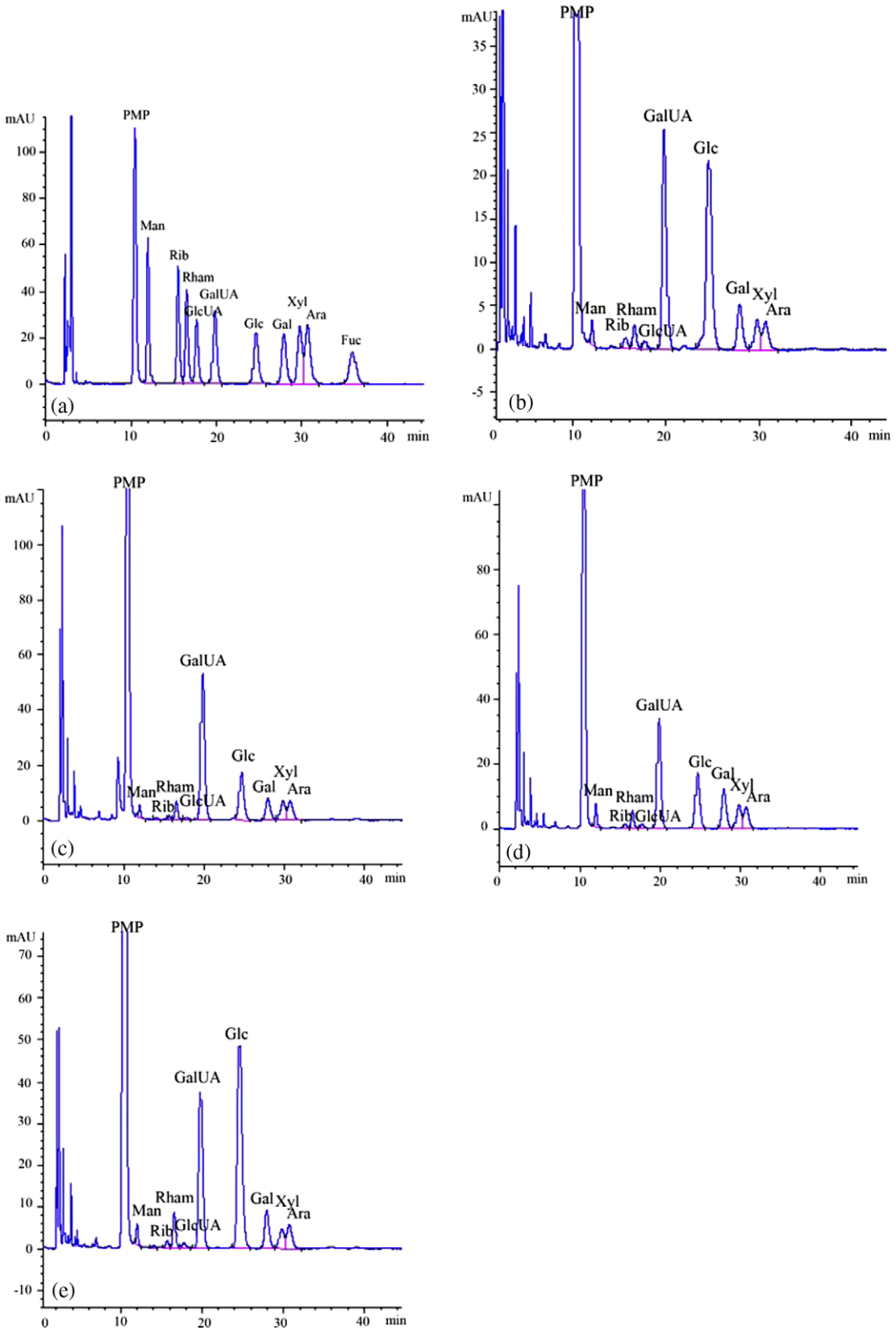

Fig. 1. HPLC images of monosaccharides from tomato CSPs (Sugars are expressed as Man, Mannitose; Rib, ribose; Rha (Rham), rhamnose; GlcUA, glucuronic aicd; GalUA, Galacturonic acid; Glc, glucose; Gal, galactose; Xyl, xylose; Ara, arabinose; Fuc, fucose.). (a) Ten standard monosaccharides; (b) 'Dongsheng' turning stage tomato; (c) 'Dongsheng' light-red stage tomato; (d) 'Geruisi' turning stage tomato; and (e) 'Geruisi' light-red stage tomato.

Table 2
Neutral sugar compositions (mg/100 g) of tomato CSP in the two cultivars and two ripening stages[e].

Monosaccharide	Turning stage 'Dongsheng'	Light-red stage 'Dongsheng'	Turning stage 'Geruisi'	Light-red stage 'Geruisi'
Man	0.922 ± 0.270b	1.021 ± 0.035b	1.589 ± 0.057a	0.992 ± 0.128b
Rib	0.507 ± 0.189a	0.454 ± 0.086a	0.476 ± 0.114a	0.619 ± 0.057a
Rha	1.372 ± 0.351c	2.621 ± 0.454ab	2.014 ± 0.293b	2.727 ± 0.025a
GlcUA	0.404 ± 0.055b	0.486 ± 0.094ab	0.633 ± 0.071a	0.478 ± 0.127ab
GalUA	15.136 ± 3.400b	22.931 ± 0.350a	14.744 ± 0.393b	15.838 ± 0.563b
Glc	4.038 ± 0.090b	3.637 ± 0.086c	4.351 ± 0.103a	3.782 ± 0.102c
Gal	3.424 ± 0.461b	3.923 ± 0.365b	6.027 ± 0.469a	4.053 ± 0.726b
Xyl	1.654 ± 0.042c	2.759 ± 0.532b	3.445 ± 0.207a	1.906 ± 0.411c
Ara	2.015 ± 0.319b	2.697 ± 0.568a	3.025 ± 0.062a	2.502 ± 0.194ab

[e] The values that have different letters in the same line are significantly ($P < 0.05$) different.

inose (Ara), xylose (Xyl) and rhamnose (Rha). Compared with the standard monosaccharides (Fig. 1a), there was no fucose (Fuc) detected from the tomato CSP, which was consistent with previous reports (Kirby et al., 2008; Lenucci et al., 2008). Both the Lenucci and Kirby groups reported that only trace of fucose existed in the whole cell walls of tomatoes. Glc, Gal, Ara, and Xyl were the main neutral sugars among these. Xyl and Gal were reported to be the most abundant noncellulosic neutral sugar components in the ethanol-insoluble fraction of ripening tomatoes, which were followed by Glc and Ara (Almeida & Huber, 2008). Our result was consistent with the report as well. For both cultivars, the Rha increased during ripening might be due to the significant degradation of RG I (Vicente, Powell, Greve, & Labavitch, 2007).

Table 2 shows that both the proportions of GalUA and Rha increased during ripening in both cultivars. The proportions of Gal, Xyl and Ara in 'Dongsheng' tomato CSP increased during ripening whereas it decreased in 'Geruisi'. The result demonstrates that the different pectin sources had different proportions of the side chains and the degree of branching (Vincken et al., 2003; Willats et al., 2001). The decreased contents of monosaccharides might be attributed to the degradation of pectin side chains rich in arabinans, galactans and arabinogalactans by the glycosidases, β-galactosidase and α-arabinofuranosidase, for instance (Tateishi et al., 2005).

Galactan and arabinan have essential roles in maintaining the structure and function of the fruit cell wall (Brummell, 2006). Table 2 shows that during ripening Gal and Ara change differently in both cultivars, they increased in 'Dongsheng' while decreased in 'Geruisi'. Although loss of polymeric Gal and Ara from the fruit cell wall was a common characteristic of fruit ripening, there was great variability among species that made it complex.

It should be noted that we have illustrated that textural differences among different ripening stages for the same cultivar are different from those among different cultivars in the similar ripening stage. The former could be from biochemical and/or enzymatic reactions, while the latter could be due to the changes of the fruit cell wall skeleton. Therefore, the current results cannot be compared directly with that of Yang and others (2009).

Based on pectin structure, the change of CSP main chains was reflected by the ratio of GalUA to Rha, and the modification of CSP side chains was reflected by the change in ratios of Gal to Rha and Ara to Rha. The ratios of GalUA to Rha, Gal to Rha and Ara to Rha of tomatoes CSP decreased during ripening, which demonstrates that though the CSP contents of tomatoes were increased, the structure of CSP was modified during ripening. These modifications of pectin are thought to exist in tomato, strawberry and many other fruits (Brummell, 2006).

3.3. Effects of ripening stages and cultivars on the nanostructures of CSP

Even though changes of chemical contents of CSP was important for illustrating the texture and softening of fruit during ripening, the changes of the fruit cell wall that were most correlated with softening was widely viewed as the depolymerisation of polysaccharide matrixs (Brummell, 2006). Therefore, it was essential to investigate and compare the nanostructure of the CSP in different ripening stages and cultivars, which could help illustrate the mechanism of softening during fruit ripening.

The plane and 3-dimensional AFM images (also zoom images) of tomato CSP in different groups are shown in Figs. 2 and 3. The effects of ripening stages and cultivars on the nanostructure of CSP could be illustrated by comparing the images within these figures. In the figures, the chains of CSP were different, which suggests that the pectin structure of tomatoes was heterogenic, this property was similar with that of peaches (Yang et al., 2006a, 2006b), apricots (Liu et al., 2009), and Chinese cherries (Zhang et al., 2008). The qualitative characteristics of the heterogeneous CSP structures, including polymers (p), long chains (lc), linear single fraction (ls), short chains (sc) and branching (br), moreover, cleavage points (cp), as well as the releasing point (rp) of pectin chains which were released from the chelator (CDTA) indicating that the degradation of CSP could be identified from the AFM images, especially from the 3-dimensional and zoom images (Yang et al., 2006b).

Compared with light-red stage tomatoes, turning stage tomatoes in both cultivars showed more polymers that entangled together (Figs. 2a and 3a). Large CSP polymers often forming a conglomerate with the chelator of CDTA (ch), as shown in Fig. 2e and f, were commonly observed. Few linear single fraction (ls), short chains (sc) could be imaged as well (e.g. in Fig. 2c). For CSP of light-red stage tomatoes, branching (br), cleavage points (cp), and the releasing point (rp) were obvious (e.g. in Figs. 2f and 3c and e). Linear single fraction (ls) and short chains (sc) were found more in both light-red stage groups than turning stage ones. The result was similar to that of CSP molecules from fresh peach fruit (Yang et al., 2006b). Furthermore, a helical structure was detected (e.g. in Fig. 2f). The extended helical structure suggests that the pectin molecules might be helical like when they were adsorbed onto the mica surface. The helix or not of the pectin chains was mainly determined by the height of the chains. Periodicity, variations and branching structures could serve as additional information for judging whether the structure is helix or not (Yang, Chen, An, & Lai, 2009). Similar behavior was observed in tomato and sugar beet pectin molecules (Kirby et al., 2008). Linear single fractions released from large polymers (e.g. in Fig. 2e) were also found in the AFM images. Compared with the 'Dongsheng' cultivar, fewer branches of CSP were observed in ripe 'Geruisi' tomatoes (e.g. in Fig. 2e). Unfortunately the process of branches detached from main chains and enzymatically hydrolyzed into small fractions was not observable by AFM, which might be due to the size limitation of small fraction.

It should be noted that pectin molecules were highly heterogeneous in nanoscale morphology, therefore, both Fig. 2a and c were typical images of turning stage group even though there was much difference between them.

The quantitative information of CSP chains could be obtained by applying the function 'section analysis' of the software (Yang et al., 2006b). For an AFM image, a cross-sectional line could be drawn across the image, the vertical profile along the line was then displayed. The cursor could be placed on the line section at any point to make horizontal, vertical and angular measurements.

Table 3 shows the statistical quantitative results of CSP chains. The widths of chains from section analysis reflect two groups of basic units (15.625, 17.578 and 23.438 nm for 'Dongsheng'; 15.625, 19.531 and 23.438 nm for 'Geruisi'), the widths of other chains were composed of these three values in both cultivars (Table 3). For example, for the 'Dongsheng' cultivar, 31.250, 35.156

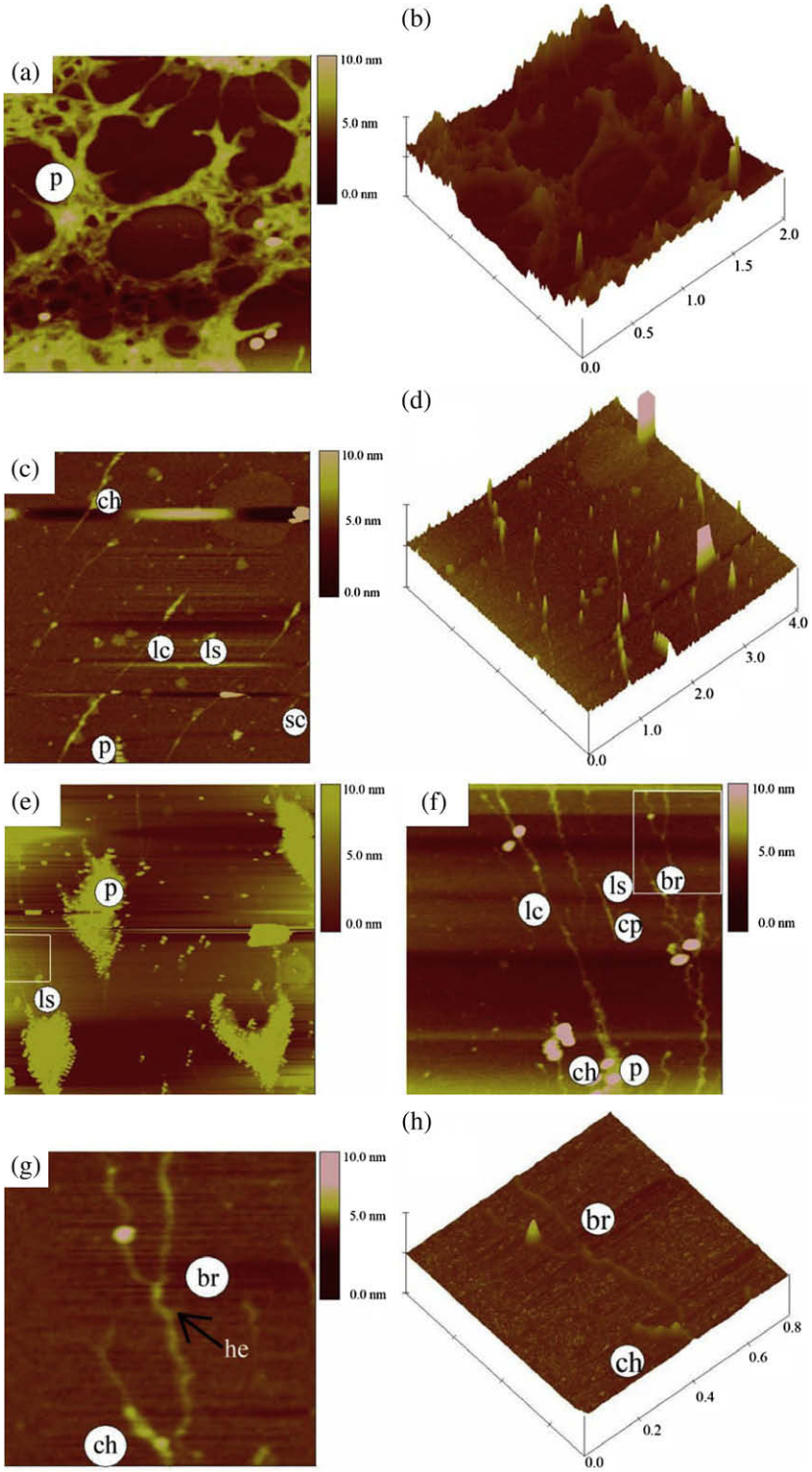

Fig. 2. AFM images of CSP from 'Dongsheng' tomato (ch, chelator (CDTA); lc, long chains; ls, linear single fractions; p, polymers; sc, short chains; br, branch structures; cp, cleavage points; he, helix structure. Height bar = 10 nm.). (a) Typical image of turning stage group, scan size: 2 × 2 μm; (b) 3-dimensional (3D) image of image (a) and (c); (d) typical plane and 3D images of turning stage group, scan size: 4 × 4 μm; (e) typical image of light-red stage group, scan size: 10 × 10 μm; (f) zoom plane image in the marked square of (e), scan size: 2 × 2 μm; (g) and (h) zoom plane and 3D image of the marked square of image (f), scan size: 0.8 × 0.8 μm.

and 46.875 nm were approximately double that of the numbers 15.625, 17.578 and 23.438 nm, respectively. 62.500 nm was approximately fourfold of 15.625 nm and two times of 31.250 nm. 39.063 nm was about the sum of 15.625 and 23.438 nm, 58.594 nm could be the addition of 23.438 and 35.156 nm, 78.125 nm was the sum of 46.875 and 31.250 nm and 117.190 nm was approximately the sum of 39.063 and 78.125 nm. The rule was also applicable for the 'Geguisi' cultivar, the only difference was the basic values. Generally, the widths of the tomatoes here were smaller than those of peaches (Yang et al., 2006b). The heights (*V*) of the tomato CSPs varied from 0.161 to 5.254 nm (Table 3), mainly between 1.0 to 3.0 nm. The heights of the tomato CSP was relatively larger than that of peaches (Yang et al., 2006b), the height of tomato CSP might not only come from the single chains, but also from the congeries which were composed of tangled single chains.

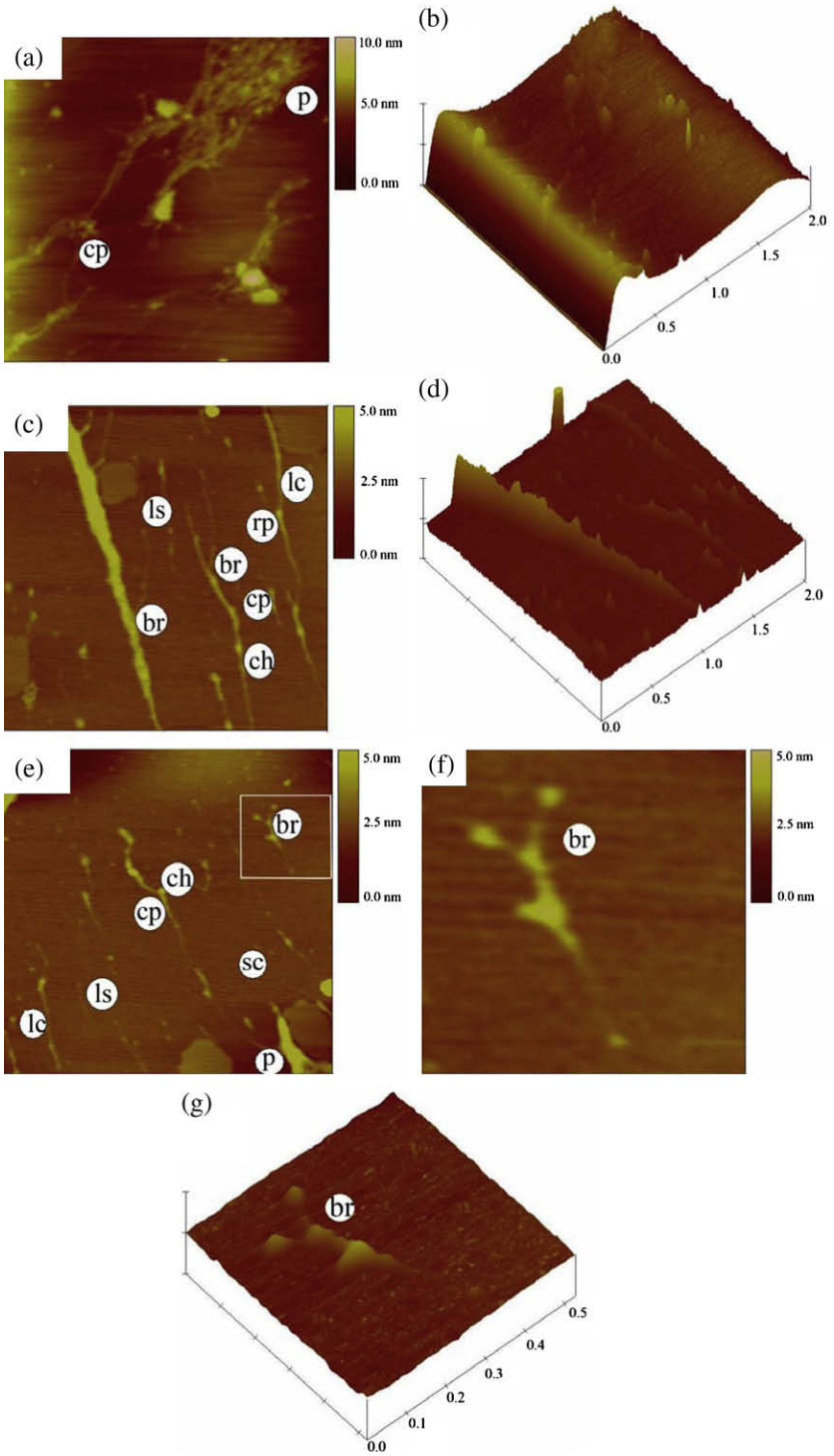

Fig. 3. AFM images of CSP from 'Geruisi' tomato (br, branch structures; ch, chelator (CDTA); cp, cleavage points; lc, long chains; ls, linear single fractions; p, polymers; sc, short chains; rp, releasing point of pectin released from the CDTA. Height bar: 10 nm for (a) and (b); 5 nm for others.). (a) and (b) Typical plane and 3D images of turning stage group, scan size: 2 × 2 μm; (c) and (d) typical plane and 3D images of light-red stage group, scan size: 2 × 2 μm; (e) another typical image of light-red stage group, scan size: 2 × 2 μm; (f) and (g) zoom plane and 3D images of the marked square of image (e), scan size: 0.5 × 0.5 μm.

Table 3
Frequency (*Fq*) and vertical distances (*V*) of chain widths (*W*) of CSP in the two cultivars and two ripening stages[a].

W (nm)	Turning stage 'Dongsheng'		Light-red stage 'Dongsheng'		Turning stage 'Geruisi'		Light-red stage 'Geruisi'	
	Fq (N (%))	*V* (nm)	*Fq* (N (%))	*V* (nm)	*Fq* (N (%))	*V* (nm)	*Fq* (*N* (%))	*V* (nm)
15.625	–	–	1(4.0)	0.461 ± 0.000	–	–	2(13.3)	0.338 ± 0.117
17.578	–	–	1(4.0)	0.392 ± 0.000	–	–	–	–
19.531	–	–	–	–	1(6.7)	0.432 ± 0.000	2(13.3)	0.161 ± 0.064
23.438	2(11.1)	0.553 ± 0.162	9(36.0)	0.571 ± 0.237	3(20.0)	0.797 ± 0.002	5(33.3)	0.486 ± 0.160
31.250	7(38.9)	1.095 ± 0.253	5(20.0)	1.272 ± 0.445	4(26.7)	1.385 ± 0.556	2(13.3)	0.478 ± 0.190
35.156	1(5.6)	1.130 ± 0.000	1(4.0)	1.082 ± 0.000	–	–	–	–
39.063	2(11.1)	1.227 ± 0.000	1(4.0)	1.671 ± 0.000	2(13.3)	0.827 ± 0.486	2(13.3)	0.458 ± 0.051
46.875	2(11.1)	1.561 ± 0.777	3(12.0)	1.246 ± 0.570	3(20.0)	1.375 ± 0.333	1(6.7)	1.299 ± 0.000
58.594	1(5.6)	3.346 ± 0.000	1(4.0)	1.271 ± 0.000	1(6.7)	1.730 ± 0.000	–	–
62.500	1(5.6)	3.547 ± 0.000	–	–	–	–	1(6.7)	1.430 ± 0.000
78.125	1(5.6)	2.559 ± 0.000	2(8.0)	0.715 ± 0.110	1(6.7)	0.342 ± 0.000	–	–
117.190	1(5.6)	5.254 ± 0.000	1(4.0)	1.231 ± 0.000	–	–	–	–

[a] *W*, the peak width of half height of CSP chains; *V*, the height of CSP chains; *Fq*, the numbers of times particular chain widths were observed.

Table 3 shows that, for both cultivars, the turning stage groups contained higher percentages of wide chains than light-red stage groups. The percents of pectin width not less than 58.594 nm in the 'Dongsheng' cultivar were 22.4 and 16.0 for turning and light-red stage groups, respectively. The percents of width not less than 46.875 nm in the 'Geruisi' cultivar were 46.7 and 26.7 for turning and light-red stage groups, respectively. The difference of the CSP chain widths between light-red and turning stage groups might be strongly related to the different enzyme activity of tomatoes during ripening (Ali, Chin, & Lazan, 2004).

During ripening, tomato experienced moderate pectin depolymerisation and solubilisation, it also experienced a low extent of Ara loss and high Gal loss (Brummell, 2006). From our current results, moderate pectin depolymerisation and solubilisation during ripening existed in both cultivars by AFM data and CSP results. However, only 'Geruisi' had the low extent of Ara loss (no significant difference between ripe and unripe groups) and high Gal loss (significant difference between ripe and unripe groups), 'Dongsheng' cultivar did not show the same changes of Ara and Gal as 'Geruisi', suggesting that the change of neutral sugar composition varied among cultivars.

4. Conclusions

Large CSP polymers of ripe tomatoes degraded more with lower firmness than unripe (turning group) tomatoes. The percentage of wide CSP chains decreased during ripening. The widths of CSP chains were composed of several units. The compositions of tomato CSP were mainly GalUA, Glc, Gal, Ara, and Xyl. It shows that the morphology of CSP was closely related with firmness in different cultivars and ripening stages but the profiles of neutral sugar compositions varied depending on cultivars. The results were helpful for illustrating the ripening process and taking corresponding measures to extend the shelf-life of postharvest fruits and vegetables.

Acknowledgment

Project 30600420 supported by National Natural Science Foundation of China contributed to this research.

References

Ali, Z. M., Chin, L. H., & Lazan, H. (2004). A comparative study on wall degrading enzymes, pectin modifications and softening during ripening of selected tropical fruits. *Plant Science, 167*, 317–327.

Almeida, D. P. F., & Huber, D. J. (2008). In vivo pectin solubility in ripening and chill-injured tomato fruit. *Plant Science, 174*, 174–182.

Artés, F., Conesa, M. A., Hernández, S., & Gil, M. I. (1999). Keeping quality of fresh-cut tomato. *Postharvest Biology and Technology, 17*, 153–162.

Bonnin, E., Dolo, E., Le Goff, A., & Thibault, J. F. (2002). Characterisation of pectin subunits released by an optimised combination of enzymes. *Carbohydrate Research, 337*, 1687–1696.

Brummell, D. A. (2006). Cell wall disassembly in ripening fruit. *Functional Plant Biology, 33*, 103–119.

Duan, X., Cheng, G., Yang, E., Yi, C., Ruenroengklin, N., Lu, W., et al. (2008). Modification of pectin polysaccharides during ripening of postharvest banana fruit. *Food Chemistry, 111*, 144–149.

Fu, D., & O'Neill, R. A. (1995). Monosaccharide composition analysis of oligosaccharides and glycoproteins by high-performance liquid chromatography. *Analytical Biochemistry, 227*, 377–384.

Getinet, H., Seyoum, T., & Woldetsadik, K. (2008). The effect of cultivar, maturity stage and storage environment on quality of tomatoes. *Journal of Food Engineering, 87*, 467–478.

Honda, S., Akao, E., Suzuki, S., Okuda, M., Kakehi, K., & Nakamura, J. (1989). High-performance liquid chromatography of reducing carbohydrates as strongly ultraviolet-absorbing and electrochemically sensitive 1-phenyl-3-methyl-5-pyrazolone derivatives. *Analytical Biochemistry, 180*, 351–357.

Javanmardi, J., & Kubota, C. (2006). Variation of lycopene, antioxidant activity, total soluble solids and weight loss of tomato during postharvest storage. *Postharvest Biology and Technology, 41*, 151–155.

Kirby, A. R., MacDougall, A. J., & Morris, V. J. (2008). Atomic force microscopy of tomato and sugar beet pectin molecules. *Carbohydrate Polymers, 71*, 640–647.

Lana, M., Tijskens, L., & Kooten, O. (2005). Effects of storage temperature and fruit ripening on firmness of fresh cut tomatoes. *Postharvest Biology and Technology, 35*, 87–95.

Lenucci, M. S., Leucci, M. R., Piro, G., & Dalessandro, G. (2008). Variability in the content of soluble sugars and cell wall polysaccharides in red-ripe cherry and high-pigment tomato cultivars. *Journal of the Science of Food and Agriculture, 88*, 1837–1844.

Lien, C. C., Ay, C., & Ting, C. H. (2009). Non-destructive impact test for assessment of tomato maturity. *Journal of Food Engineering, 91*, 402–407.

Liu, H., Chen, F., Yang, H., Yao, Y., Gong, X., Xin, Y., et al. (2009). Effect of calcium treatment on nanostructure of chelate-soluble pectin and physicochemical and textural properties of apricot fruits. *Food Research International, 42*, 1131–1140.

Martínez-Romero, D., Guillén, F., Castillo, S., Zapata, P. J., Valero, D., & Serrano, M. (2009). Effect of ethylene concentration on quality parameters of fresh tomatoes stored using a carbon-heat hybrid ethylene scrubber. *Postharvest Biology and Technology, 51*, 206–211.

Mizrach, A. (2007). Nondestructive ultrasonic monitoring of tomato quality during shelf-life storage. *Postharvest Biology and Technology, 46*, 271–274.

Muskovics, G., Felföldi, J., Kovács, E., Perlaki, R., & Kállay, T. (2006). Changes in physical properties during fruit ripening of Hungarian sweet cherry (*Prunus avium* L.) cultivars. *Postharvest Biology and Technology, 40*, 56–63.

Ovodova, R. G., Popov, S. V., Bushneva, O. A., Golovchenko, V. V., Chizhov, A. O., Klinov, D. V., et al. (2006). Branching of the galacturonan backbone of comaruman, a pectin from the marsh *Cinquefoil Comarum palustre L. Biochemistry (Moscow), 71*, 538–542.

Round, A. N., Rigby, N. M., MacDougall, A. J., Ring, S. G., & Morris, V. J. (2001). Investigating the nature of branching in pectin by atomic force microscopy and carbohydrate analysis. *Carbohydrate Research, 331*, 337–342.

Saliba-Colombani, V., Causse, M., Langlois, D., Philouze, J., & Buret, M. (2001). Genetic analysis of organoleptic quality in fresh market tomato. 1. Mapping QTLs for physical and chemical traits. *Theoretical and Applied Genetics, 102*, 259–272.

Tateishi, A., Mori, H., Watari, J., Nagashima, K., Yamaki, S., & Inoue, H. (2005). Isolation, characterization, and cloning of α-L-arabinofuranosidase expressed during fruit ripening of Japanese pear. *Plant Physiology, 138*, 1653–1664.

Vicente, A. R., Powell, A., Greve, L. C., & Labavitch, J. M. (2007). Cell wall disassembly events in boysenberry (*Rubus idaeus* L. × *Rubus ursinus* Cham. & Schldl.) fruit development. *Functional Plant Biology, 34*, 614–623.

Vincken, J. P., Schols, H. A., Oomen, R. J. F. J., McCann, M. C., Ulvskov, P., Voragen, A. G. J., et al. (2003). If homogalcturonan were a side chain of rhamnogalacturonan I. Implications for cell wall architecture. *Plant Physiology, 132*, 1781–1789.

Willats, W. G. T., McCartney, L., Mackie, W., & Knox, J. P. (2001). Pectin: cell biology and prospects for functional analysis. *Plant Molecular Biology, 47*, 9–27.

Yang, H., Feng, G., An, H., & Li, Y. (2006a). Microstructure changes of sodium carbonate-soluble pectin of peach by AFM during controlled atmosphere storage. *Food Chemistry, 94*, 179–192.

Yang, H., Lai, S., An, H., & Li, Y. (2006b). Atomic force microscopy study of the ultrastructural changes of chelate-soluble pectin in peaches under controlled atmosphere storage. *Postharvest Biology Technology, 39*, 75–83.

Yang, H., Chen, F., An, H., & Lai, S. (2009). Comparative studies on nanostructures of three kinds of pectins between two cultivar peaches using atomic force microscopy. *Postharvest Biology and Technology, 51*, 391–398.

Zhang, L., Chen, F., An, H., Yang, H., Sun, X., Guo, X., et al. (2008). Physicochemical properties, firmness, and nanostructures of sodium carbonate-soluble pectin of 2 Chinese cherry cultivars at 2 ripening stages. *Journal of Food Science, 73*, N17–N22.